Desalination and Water Treatment
www.deswater.com

doi: 10.1080/19443994.2016.1193061

57 (2016) 28875–28886
December

Taylor & Francis
Taylor & Francis Group

Green synthesized Fe_3O_4 nanoparticles as a magnetic core to prepare poly 1, 4 phenylenediamine nanocomposite: employment for fast adsorption of lead ions and azo dye

Mostafa Hossein Beyki[a], Mahsa Shirkhodaie[a], Mohammad Ali Karimi[b], Mohammad Javad Aghagoli[a], Farzaneh Shemirani[a,*]

[a]*School of Chemistry, University College of Science, University of Tehran, P.O. Box 14155-6455, Tehran, Iran, Tel. +98 21 61112481; Fax: +98 21 66405141; emails: hosseinbakim@gmail.com (M. Hossein Beyki), m.shirkhodaie@gmail.com (M. Shirkhodaie), j.aghagoli@ut.ac.ir (M.J. Aghagoli), Shemiran@khayam.ut.ac.ir (F. Shemirani)*

[b]*Faculty of Medical Sciences, Department of pharmacology and toxicology, Kerman, Iran, email: mohamadalikarimi2000@yahoo.com*

Received 18 December 2015; Accepted 19 May 2016

ABSTRACT

Different approaches such as precipitation, combustion, and hydrothermal method are available to prepare Fe_3O_4 nanoparticles. Respect to other methods, precipitation, especially with one iron source and natural reducing agents is a more green, economic, fast, and simple route for Fe_3O_4 synthesis. Based on these viewpoints, we have prepared Fe_3O_4 magnetic nanoparticles via a sonochemistry precipitation method using only one iron source and sugar, which was employed as a reducing agent. The combination of these prepared magnetic nanoparticles with polyphenylenediamine via an emulsion polymerization resulted in a magnetic polymer nanocomposite. The prepared magnetic material was characterized by Fourier transform infrared (FT-IR), scanning electron microscope (SEM), transmission electron microscopy (TEM), X-ray powder diffraction (XRD), and vibration sample magnetometer techniques. The magnetic nanocomposite was then successfully employed as an adsorbent in the removal of Pb^{2+} ions and Direct red 81 (DR-81) from single and binary solution. The results demonstrated that the maximum adsorption was obtained within 5 min at pH 4.0 and also the adsorption processes of Pb^{2+} and DR-81 both were well fitted by pseudo-second-order kinetic model. The experimental data were analyzed by the Langmuir and Freundlich adsorption models. Freundlich model provided the best correlation of the experimental data for dye but lead adsorption well fitted with Langmuir model. Moreover, the maximum capacity of polymer nanocomposite was found to be 144.92 and 370.37 mg g^{-1} for DR-81 and Pb^{2+}, respectively.

Keywords: Dye; Lead; Magnetic nanocomposite; Polymer

1. Introduction

It goes without saying that iron oxide nanoparticles are one of the most-studied materials in the wastewater treatment owing to low toxicity; biocompatibility; high specific surface favors the binding efficiency; low mass transfer resistance, magnetic separation under a magnetic field; as well as low operation cost. However, the problems of aggregation and rapid biodegradation have limited applications of

*Corresponding author.

magnetic nanoparticles as an adsorbent [1–4]. With this in mind, nanomaterials based on polymers not only are able to provide favorable functional groups for various applications but also could decrease the aforementioned problems. It is worth noting that amine-containing conductive polymers have attracted a great deal of attention in recent years due to their excellent chemical and physical properties originating from the π-conjugated system [5–7]. As a diamine derivative of polyaniline, which has higher content of functional groups in conjugated structure and more intriguing multi-functionality among the conjugated polymers, poly phenylenediamine, a cost effective polymer, shows exceptional prospects in such applications as waste—water treatment [8,9]. Furthermore, its effective adsorption performance as an adsorbent in removing heavy metal ions such as lead and azo dyes has made it to be promising adsorption materials as it bears redox properties, powerful chelation ability, and high stability at ambient conditions [9–11]. Nevertheless, conductive polymers always have small specific surface areas, which can be improved by its combination with magnetic nanoparticles. It provides robust adsorbent with improved qualities [12].

Various chemical methods such as precipitation, sol–gel, hydrothermal, and combustion are available to prepare Fe_3O_4 nanoparticles. In this regard, it is more economical to utilize one iron source. However, the employment of toxic reducing reagents has limited widespread application of the synthetic routes [13]. Biogenic synthesis of magnetic nanoparticles using green reagent with natural source is environmentally affordable. Based on this viewpoint, in this study, Fe_3O_4 nanoparticles have been synthesized through precipitation rout using one iron source and sugar as reducing agent then p-phenylenediamine@Fe_3O_4 nanocomposite were prepared by emulsion method in which particles transferred into micelles through the surfactant template and increased the molecular weight [14–16]. Combining the advantages of Fe_3O_4 and conductive polymer resulted in a promising adsorbent. Hence, its potential applications on the adsorption of direct red 81 and lead ions in a single and binary system have been demonstrated. The effect of various experimental parameters has also been studied. To evaluate the experimental data, kinetics, and adsorption isotherms models have been investigated.

2. Experimental

2.1. Materials and instrumentation

P-phenylenediamine (PDA), potassium persulfate (KPS), sodium dodecyl sulfate (SDS), chloroform, HCl, NaOH, and $Fe(NO_3)_3{\cdot}9H_2O$ (Merck, Darmstadt, Germany) have been used for the synthesis of magnetic nanoparticles and polymer nanocomposite. White sugar was supplied from a local market in Tehran. The Direct Red-81 (DR-81) which was used as a model dye was supplied from chemistry & chemical engineering research center of Iran. The stock dye solution was prepared by dissolving an appropriate amount of dye powder in distilled water. Lead standard solution (1000 mg L^{-1}) was obtained by dissolving $Pb(NO_3)_2$ salt in distilled water. The FT-IR study of the samples was done by Equinox 55 Bruker with ATR method over the wavelength of 400–4000 cm^{-1}. The SEM (model KYKY-3200, Beijing, China) and TEM (Zeiss-EM10C) was used to investigate morphology of the composite. XRD measurements were performed using an STADI-MP from an STONE company (Germany) with monochromatized Cu Kα radiation. Magnetization investigation was done using a vibration sample magnetometer (VSM) (Lake Shore Model 7400, Japan). The N_2 adsorption—desorption isotherm was measured on a Nova Station A system. The pH-Meter model 781 from Metrohm (Herisau, Switzerland) equipped with glass combination electrode was used for the pH measurements. The adsorption studies of the dye and lead solutions were carried out using UV–vis spectrophotometer (Lambda 25, Perkin Elmer) and flame atomic absorption spectrometer (FAAS, Varian-400, Musgrave, Australia).

2.2. Preparation of Fe_3O_4 magnetic nanoparticles

Fe_3O_4 nanoparticles (NPs) were synthesized through an ultrasound assisted coprecipitation method using only one iron source and natural reducing agent. In a typical experimental procedure, 1.5 g of $Fe(NO_3)_3{\cdot}9H_2O$ was added into 10 ml of solution containing 0.2 g of sugar. The mixture was stirred at 60˚C. After 30 min of stirring, the solution was purged with Ar stream for 5 min to remove dissolved oxygen. Then 1.0 ml of NH_3 (25%) was added dropwise into the mixture under ultrasound radiation and the mixture was heated at 80˚C under Ar atmosphere for about 30 min. The color of resultant mixture turned into black which indicated the formation of magnetic Fe_3O_4. Then, the solution was cooled to room temperature and obtained the black product was isolated by applying an external magnetic field, washed with distilled water. Then, dried in an oven at 80˚ for 4 h and stored for further use.

2.3. Synthesis of polymer@Fe_3O_4 nanocomposite

Polymer@Fe_3O_4 nanocomposite were synthesized via an emulsion polymerization at room temperature.

Solution of 1.0 g of PDA (monomer) in 30 ml of HCl (1.0 mol L^{-1}) was added to the mixture of 0.7 g of prepared Fe_3O_4 nanoparticles, 2.5 g SDS, and 20 ml chloroform. The resulted mixture was dispersed by an ultrasonic bath at room temperature for about 1 h. Then, the fresh KPS solution (1.5 g in 20 ml distilled water) was dropped into the stirring reaction medium for 30 min. The reaction was carried out after being stirred at room temperature for about 24 h afterwards, the mixture was poured into acetone to terminate the reaction. The prepared black precipitate was filtered and washed several times with distilled water and methanol for once. At the end, it dried at 50°C for 24 h.

2.4. Adsorption procedure

For each experimental run, about 20 mg of prepared nanocomposite was added to 50 ml of Pb^{2+} ions or Direct Red-81 solution of known concentration. After adjustment of optimum pH to 4.0 using HCl and NaOH solution (0.1 mol L^{-1}), it was shaken for 5 min to reach the equilibrium. At the end of the adsorption period, by applying magnetic field, the dye solution was separated from adsorbent. Then, the concentration of residual direct red-81 and Pb^{2+} was determined by measuring the absorbance at 509.73 nm using a UV–vis spectrophotometer and FAAS, respectively. For coadsorption in binary systems, 20 mg of adsorbent was added to the mixture of DR-81 and Pb^{2+} with the different initial concentrations. The procedure of adsorption was also the same as the single analyte solution. The absorption capacity can be expressed by the following equation:

$$Q_e = (C_i - C_e)V/m \quad (1)$$

where C_i and C_e (mg L^{-1}) are initial and equilibrium liquid-phase concentration of target analyte, respectively. V is the volume of the solution (L), and m is the weight (g) of the adsorbent.

3. Results and discussion

3.1. Characterization of polymer@Fe_3O_4 nanocomposite

The SEM analysis gives a sufficient general overview of the adsorbent. Fig. 1(a) and (b), show the SEM images of synthesized Fe_3O_4 and polymer nanocomposite. The image of nanoparticle exhibits the spherical particles with a mean diameter of 30 nm. As it is illustrated, the magnetic polymer shows some agglomeration and increases in particle sizes. The TEM image (Fig. 1(c)) was also employed for further characterization of the nanocomposite. It is obvious that the magnetic nanoparticles are appeared as dark spots in composite structure, owing to dispersion in polymer matrices. Fig. 1(d) shows XRD patterns of the nanoparticles and polymer nanocomposite. It is found that all the reflection peaks at (1 1 1), (2 2 0), (3 1 1), (4 0 0), (4 2 2), (5 1 1), (4 4 0) can be well indexed to the inverse cubic spinel structure of Fe_3O_4. Moreover, the pattern of nanocomposite exhibits new peaks at $2\theta^\circ = 10.12$, 15.49, 20.26, and 24.0 due to crystallinity of (0 0 1), (1 0 0), (1 1 0), and (1 1 1) planes of polymer [17].

According to Fig. 2(a) which shows the FT-IR spectra of the nanoparticles, characteristic bands from Fe-O stretching vibrations are observed at 466–565 cm^{-1}. Also, the spectrum of the composite is dominated by the bands of the polymer and showed peaks at 2,919, 1,571, and 1,400–1,500 cm^{-1}, which assigned to C–H stretching, N–H-bending unit, and aromatic backbone vibration, respectively. The magnetic property of the prepared composite was carried out using a VSM at room temperature. Fig. 2(b) reveals that the values of saturation magnetization of the particle and polymer are 40.8 and 24.5 emu g^{-1} respectively. The quench in the magnetic moment for polymer nanocomposite is due to the existence of polymer on the surface of magnetic particles.

3.2. Effect of pH on Pb^{2+} and DR-81 adsorption

The initial pH solution, which is one of the most effective parameters, controls the adsorption process in that the charge of the adsorbate and adsorbent often depends on the pH of the solution. The variation of Pb^{2+} and DR-81 adsorption on the polymer@Fe_3O_4 nanocomposite at various solution pH values are shown in Fig. 3(a). As it can be seen adsorption capacity of both analytes increases with the increase in pH form 2 to 6. By increasing pH, concentration of H^+ ions get decreased. Consequently, the competition between H^+ and heavy metal cations was reduced. In other words, in the acidic media, the amine groups of adsorbent are protonated. It is worth noting that protonated cannot make a chelate to Pb^{2+} ions. At high pH (>7.0), the metal ions could precipitate as hydroxide form which leads to the decrease in removal efficiency.

It should also be noted that π–π interaction can be a main mechanism for dye adsorption as the structure of polymer and DR-81 both are composed of benzene ring (Scheme 1). Electrostatic interaction between anionic dye and positively charged adsorbent may also be proposed as another mechanism. However, by the

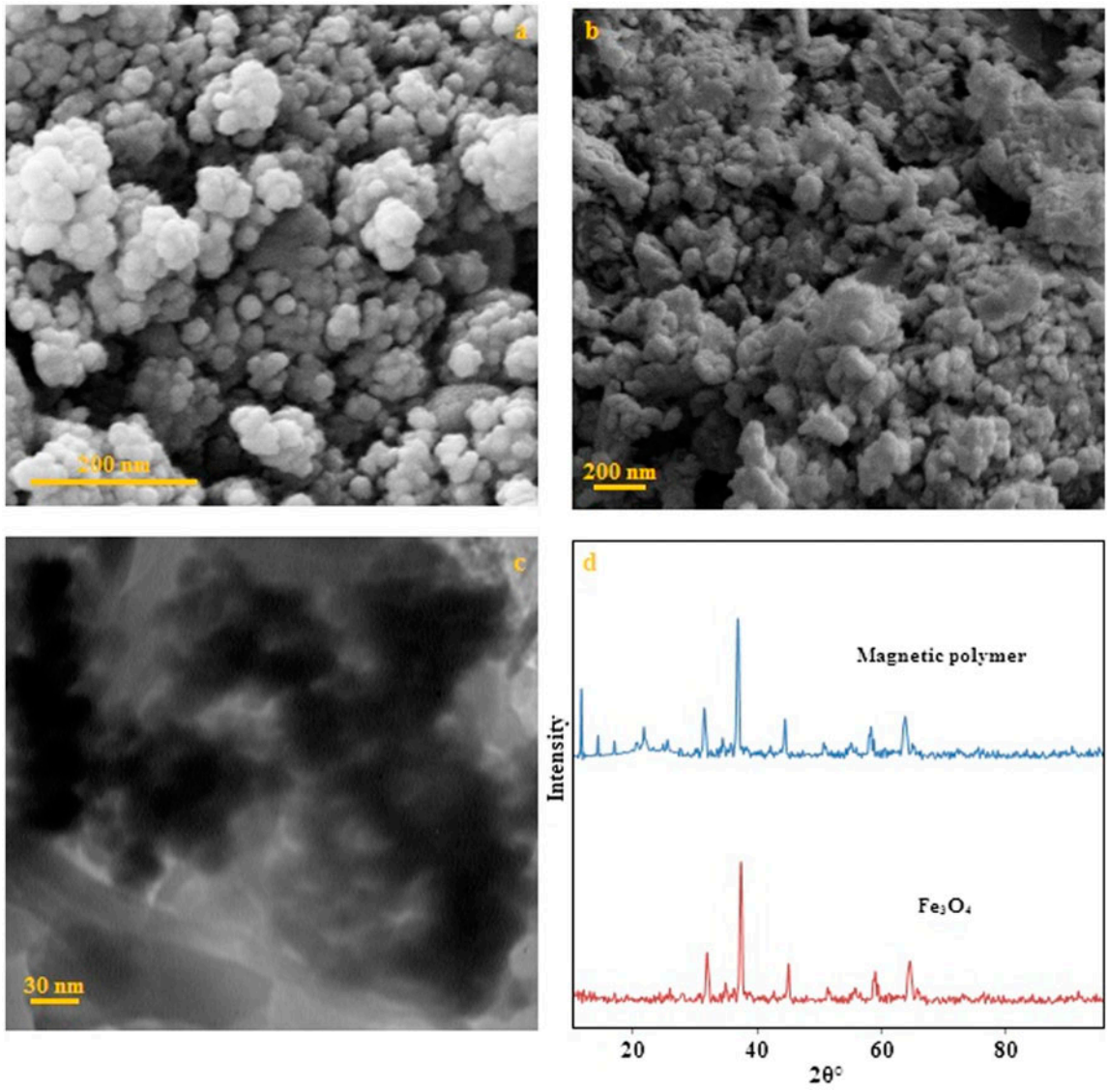

Fig. 1. SEM image of Fe_3O_4 (a), and polymer nanocomposite (b), the TEM image of polymer nanocomposit (c), and XRD pattern of nanoparticles and the composite (d).

increase in pH value adsorption efficiency increases for dye removal, which is in contrast with the estimation. This situation can be due to the fact that in acidic solution, functional group of DR-81 is in positive state and the electrostatics repulsion of the dye and positively charged sorbent resulted in the declined removal efficiency. Therefore, a pH value of 4.0 was found to be an optimum pH for the simultaneous adsorption of Pb^{2+} and DR-81.

3.3. Effect of time

Another significant parameter leading to an efficient analyte adsorption is time which should be long enough to let a complete uptake happen and also short enough to lead a time saving and cost effective adsorption step. To investigate the effect of the time on the adsorption efficiency, stirring time between 1.0 and 10 min were tested. Results, which are depicted in Fig. 3(b), showed that lead ions were efficiently removed from solution at first one min and reached equilibrium after 5 min. Moreover, the result for dye removal revealed that time of 5.0 min can also be accepted as equilibrium time. Initial fast removal is due to the availability of a large number of adsorption sites (N–H, O–H and aromatic ring) in other words; such a fast adsorption rate could be attributed to the external surface adsorption, and the absence of

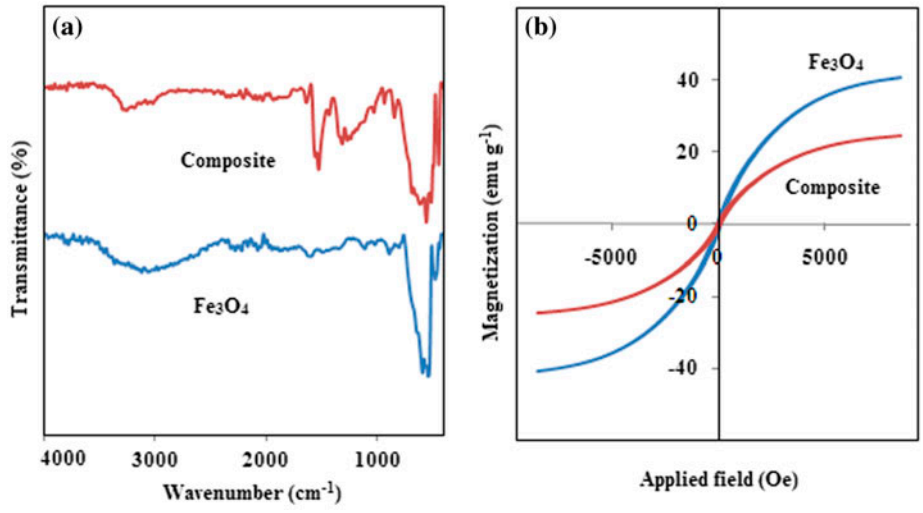

Fig. 2. FT-IR spectra (a) and VSM graph (b) of prepared materials.

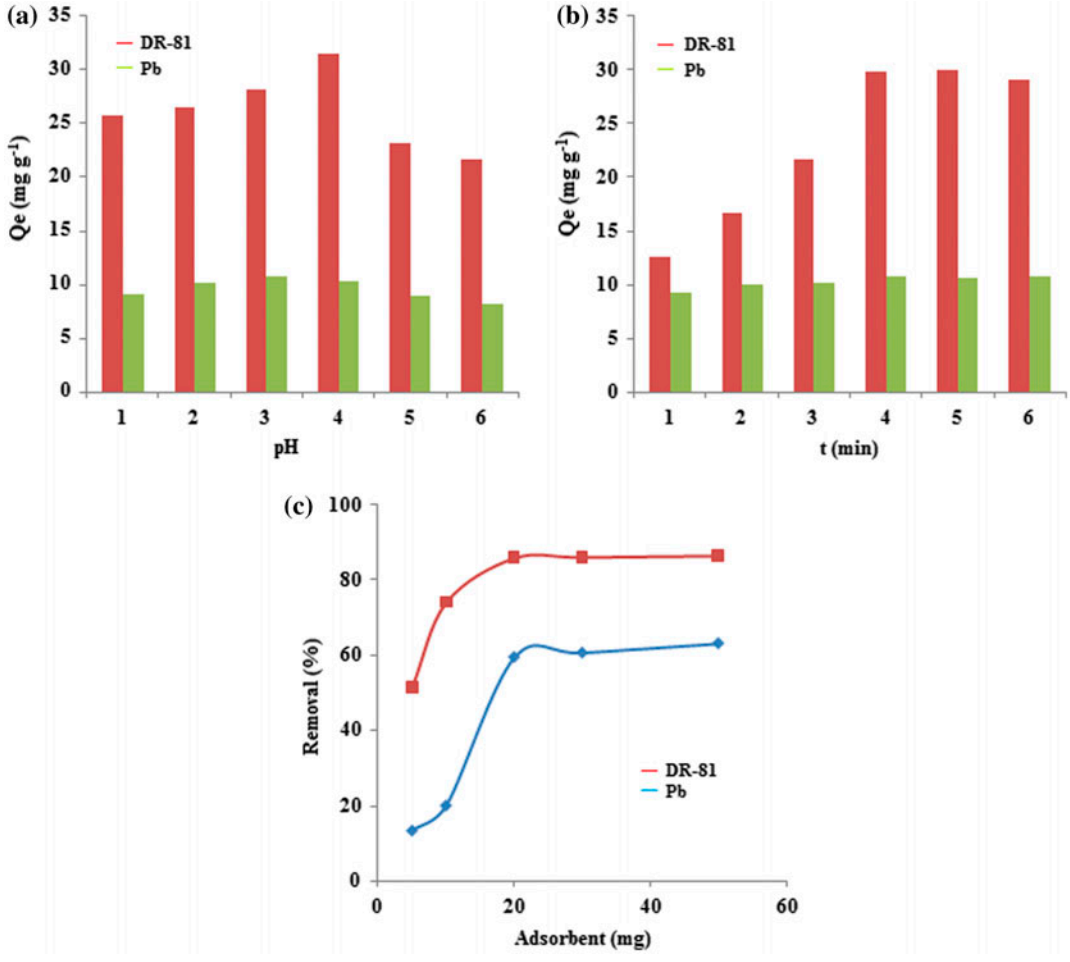

Fig. 3. Effect of pH (a), contact time (b), and adsorbent dosage (c) on lead and dye adsorption.

internal diffusion resistance. This result can be proved based on the surface area (BET) and pore volume study. The nanocomposite show low surface area (5.7 $m^2\ g^{-1}$) and low pore volume (0.02 $cm^3\ g^{-1}$) which indicated that the material has low porosity and functional groups are easily accessible to capture the analytes.

3.4. Effect of adsorbent dosage

Different dosages of magnetic nanocomposite from 10 to 50 mg were tested for the adsorption of azo dye and Pb(II) at the constant concentration and optimum pH. To do so, general procedure was applied and supernatant was analyzed to determine the amounts of remaining analytes. The results showed (Fig. 3(c)) that adsorption yield percentage increased rapidly by increasing the adsorbent dosage up to 20 mg due to the higher number of adsorption site. However, a further increase from 20 to 50 mg did not make any change in adsorption yield percentage of the analyst. This situation can be justified by the fact that high dosage may result in aggregation of the adsorbent which causes removal efficiency to reach a plateau. In other words, increasing adsorbent dosage causes the overlapping of the adsorption sites which imposes a screening effect of the dense outer layer of the particles, thereby shielding the binding sites from analyte. Excess amount of adsorbent is not economical. Therefore, the optimum amount of adsorbent was chosen to be 20 mg and further extraction experiments were carried out with the optimum amount of it.

3.5. Kinetic models

The effect of stirring time on the adsorption of dye and Pb^{2+} ions were investigated using several kinetic models under optimum conditions. Four of the main kinetic models proposed in literature were applied to the experimental data to determine the kinetic parameters and investigate the mechanism of adsorption of dye and lead by magnetic nanocomposite. The linear form of integrating the Lagergren pseudo-first-order equation, the most widely used procedures for the adsorption of solute from aqueous solution, is expressed as follows:

$$\ln(Q_e - Q_t) = \ln Q_e - k_1 t \tag{2}$$

where k_1 is the pseudo-first-order adsorption rate constant and Q_e, Q_t is the values of the amount adsorbed per unit mass at equilibrium and at any time t (mg g^{-1}) [18,19]. The values of Q_e and k_1 (mg g^{-1} min^{-1}) can be determined experimentally by plotting the $\ln(Q_e - Q_t)$ vs. t (Fig. 4(a) and (b)).

Pseudo-second-order kinetics, which is in agreement with chemisorption being the rate controlling step, is presented by Eq. (3):

$$t/Q_t = 1/k_2 Q_e^2 + t/Q_e \tag{3}$$

where k_2 (mg g^{-1} min^{-1}) is the pseudo-second-order rate constant of adsorption [20–22]. The equilibrium adsorption capacity (Q_e) and k_2 can be found experimentally from the slope and intercept of plot t/Q_t vs. t (Fig. 4(c) and (d)).

To investigate the intraparticle diffusion mechanism and its possible rate-controlling, kinetic results were analyzed by using the intraparticle diffusion model by the following equation:

$$Q_t = k_p t^{1/2} + C \tag{4}$$

where k_p represents intraparticle diffusion rate constant (mg g^{-1} min^{-1}), and C is a constant (mg g^{-1}) which gives information about the thickness of boundary layer. The plot of Q_t against $t^{1/2}$ yields a straight line passing through the origin in case of intraparticle diffusion (Fig. 5(a) and (b)).

The liquid film diffusion model, which explains the role of transport of the adsorbate from the liquid phase up to the solid-phase boundary, can be expressed as follows:

$$\ln(1 - F) = -k_{fd} t \tag{5}$$

where F is the fractional attainment of equilibrium ($F = Q_t/Q_e$) and k_{fd} is the adsorption rate constant. A linear plot of $-\ln(1 - F)$ vs. t with zero intercept would suggest that the kinetic of the sorption process is controlled by diffusion through the liquid film surrounding the solid sorbents [23]. The plot of $-\ln(1 - F)$ vs. t is illustrated in (Fig. 5(c) and (d)).

As the results indicate in Table 1, for the adsorption of DR-81 and Pb^{2+}, although pseudo-first-order plots for both of analytes are linear, this model could not describe the kinetics of adsorption of them since there was a difference between the experimental Q_e value and that obtained from the Lagergren plot for both analytes.

The second-order plots of t/Q_e versus t for both investigated analytes were also linear; moreover, the theoretical Q_e of both DR-81 and Pb^{2+} were close to their experimental values, thus this model could be

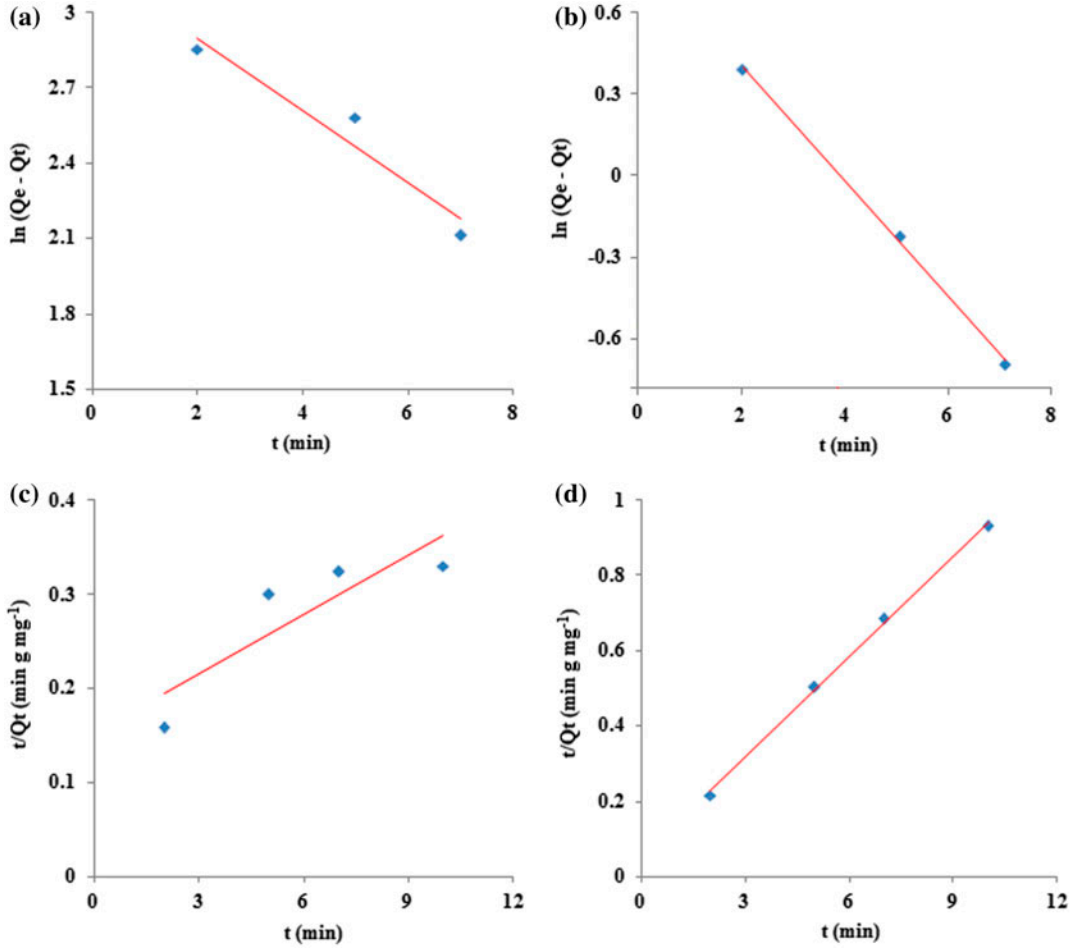

Fig. 4. First-order kinetic plot for lead (a) and DR-81 (b), and second order model plot for lead (c), and DR-81 (d) using the nanocomposite.

the best for describing the kinetics of adsorption of both of them.

The high linearity of the intraparticle diffusion plot for the adsorption of both analytes indicated that the intraparticle diffusion occurred. The line of their plots did not pass through an origin, and thus, it was not the only rate-limiting parameter.

The possibility of the film diffusion process was investigated by plotting $-\ln(1-F)$ vs. t. As can be seen, the curve exhibited linear plot with a correlation coefficient value of 0.99 and nonzero intercept. This proved the role of film diffusion in the adsorption of Pb^{2+}, although the nonzero intercept limited applicability of this model. The correlation coefficient of the plot of $-\ln(1-F)$ versus t for DR-81 was not high enough (0.93), thus this model could not describe the adsorption of DR-81 on magnetic nanocomposite.

3.6. Adsorption isotherms

Adsorption isotherms could be helpful for describing how the adsorbate molecules distribute between the liquid and the solid phase under the optimum condition when the adsorption process reaches an equilibrium state. In this study, the Langmuir and Freundlich models were used to simulate DR-81 and Pb^{2+} adsorption isotherm. Freundlich isotherm describes that adsorption occurs on a heterogeneous surface and hence does not assume monolayer capacity. The adsorption occurs at sites with different energies, and the energy of adsorption varies as a function of surface coverage [24,25]. The Freundlich isotherm is commonly expressed as follows:

$$\log Q_e = \log K_f + 1/n \log C_e \quad (6)$$

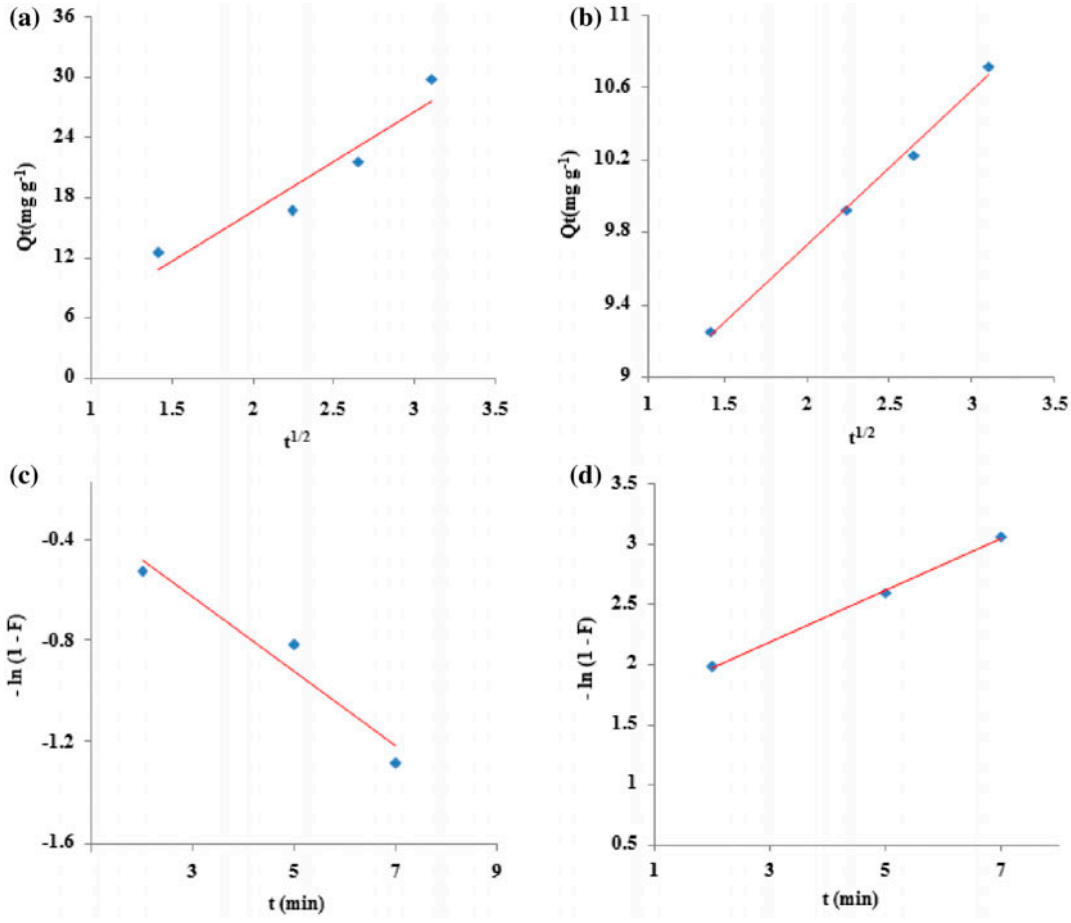

Fig. 5. The intraparticle diffusion model for lead (a), and DR-81 (b), and liquid film diffusion model for lead (c), and DR-81 (d) using the polymer nanocomposite.

Table 1
Kinetic data model for the adsorption of lead ions and DR-81 using magnetic nanocomposite

	Pseudo-first-order			Pseudo-second-order			Intraparticle diffusion		Liquid film diffusion	
	Q_e (mg g^{-1})	R^2	K_1	Q_e	R^2	K_2	K_p	R^2	K_{fd}	R^2
DR-81	24.26	0.929	0.1443	29.15	0.925	0.011	7.048	0.97	5.5	0.937
Pb^{2+}	2.291	0.99	0.2154	10.66	0.99	0.2904	0.7959	0.99	1.7	0.998

where K_f and n are calculated from the intercept and slope of the linear plot of log Q_e versus C_e (Fig. 6(a) and (b))

The Langmuir model assumes that adsorption occurs at specific homogeneous monolayer surface containing sites with uniform energy, and there is no interaction between adsorbate molecules. After completion of adsorbed monolayer, saturation of active sites occurs. Therefore, the adsorption of adsorbate stops, and no more interaction takes place between the adsorbent and adsorbate molecule [26–29].

The linear Langmuir isotherm equation can be written as followed:

$$C_e/Q_e = C_e/Q_m + \frac{1}{Q_m K_a} \quad (7)$$

where C_e is the equilibrium concentration (mg L^{-1}), Q_e is the amount adsorbed analyte at equilibrium (mg g^{-1}), Q_m is the maximum adsorption capacity of a monolayer (mg g^{-1}), and K_a is the energy of adsorption (Langmuir

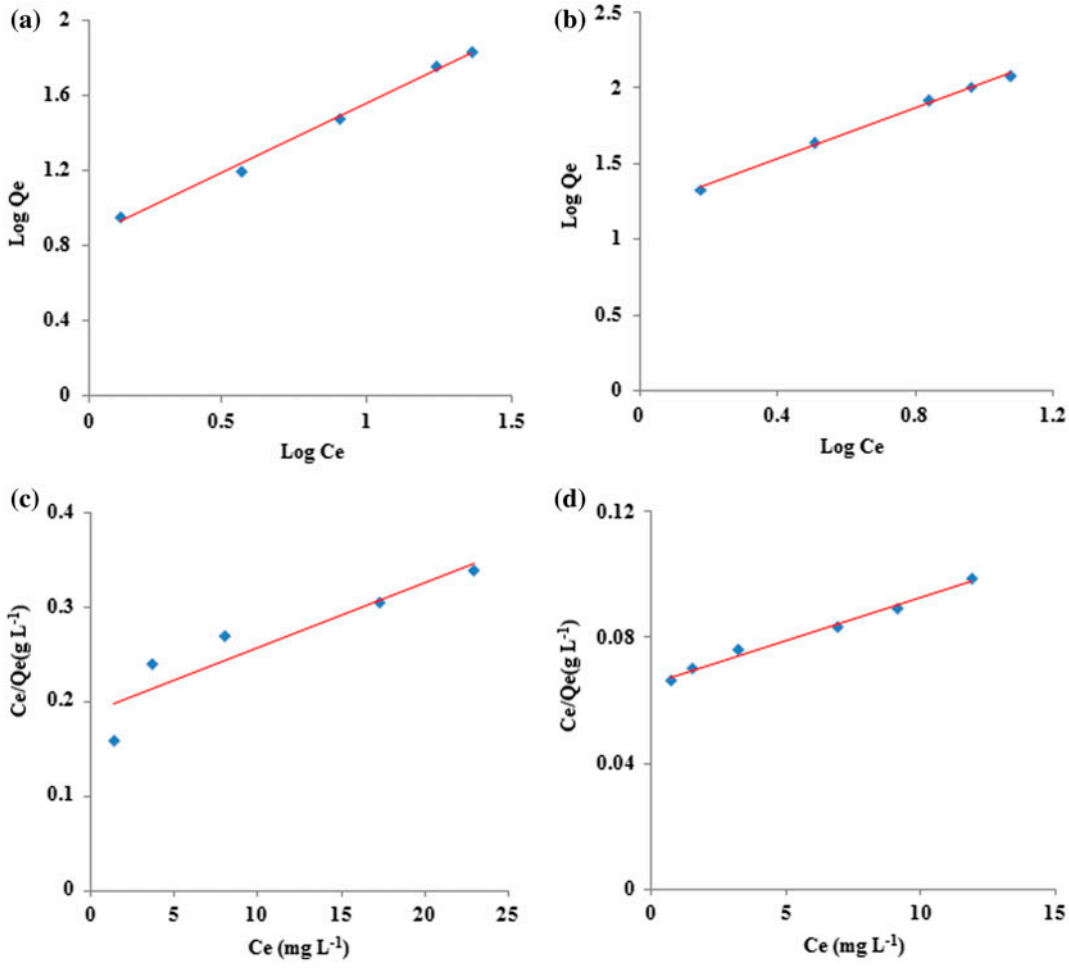

Fig. 6. The Freundlich adsorption model for lead (a), and DR-81 (b), and Langmuir isotherm model for lead (c), and DR-81 (d).

constant, L mg^{-1}). The values of Q_m and K_a were calculated from the slope and intercept of the plot of C_e/Q_e vs. C_e (Fig. 6(c) and (d)). The value of the dimensionless parameter R_L which is the measure of adsorption favorability is calculated according to Eq. (8):

$$R_L = 1/(1 + C_o K_a) \tag{8}$$

The R_L value was found in the range of $0 < R_L < 1$ which indicated a favorable adsorption process.

It is necessary to fit the equilibrium adsorption data to analyze an adsorption process, and hence, the chi-square test (χ^2) was used to test the accuracy of the isotherm models [30]:

$$\chi^2 = \sum \frac{(Q_{exp} - Q_c)2}{Q_c} \tag{9}$$

where Q_{exp} and Q_c are the experimental data and the calculated from nonlinear models. According to the results, Fig. 7 and Table 2, the Freundlich model had better linearity for both analytes, but error analysis for lead ions confirms that Langmuir model showed lower χ^2 value; and hence, Langmuir model can better describe adsorption behavior of the lead ions. The error analysis for DR-81 exhibited that the experimental data well fitted with Freundlich model, which confirmed the result of the linear isotherm model.

3.7. Mutual adsorption result

In one binary system, the initial concentration of DR-81 was fixed to 20 mg L^{-1}, whereas the concentration of Pb^{2+} was varied. The effect of Pb^{2+} concentration on DR-81 adsorption is depicted in Fig. 8. It can be seen that increases of Pb^{2+} concentration, decreased

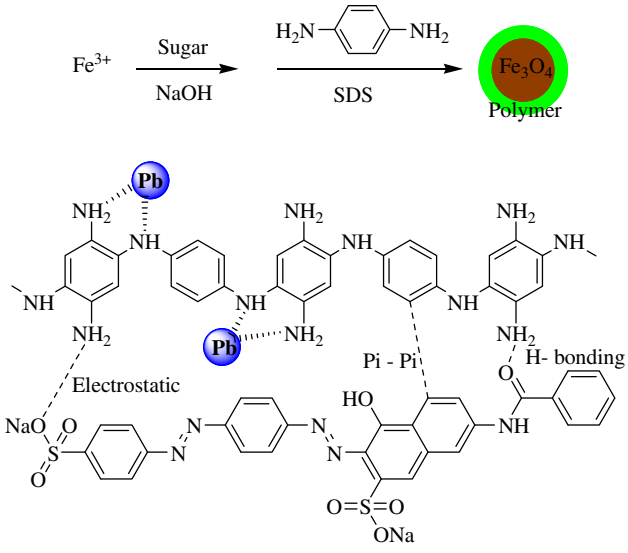

Scheme 1. Proposed mechanism for dye and metal adsorption bye the polymer nanocomposite.

the adsorption of DR-81. The adsorption capacities for DR-81, decreased from 29.3 to 13.3 mg g^{-1} (reduction of 54.6%) in the presence of Pb^{2+}. Hence, there is the competitive between the adsorption of metal ion and anionic dye and the nanocomposite has a better affinity for Pb^{2+} ions. This indicates that active sites for both analytes are similar. In other words, owing to lower size of lead ions compared to dye molecules, it easily diffuses in the adsorbent structure and reacts with amine and hydroxyl functional groups. Occupation of active sites with lead ions causes less interaction between dye and adsorbent surface as a result dye removal efficiency decreases. In order to investigate the effect of DR-81 concentration on Pb^{2+} adsorption in another binary system, the initial

Table 2
Isotherm data for adsorption of lead ions and DR-81 using magnetic nanocomposite

Langmuir	DR-81	Pb^{2+}	Freundlich	DR-81	Pb^{2+}
R^2	0.84	0.98	R^2	0.99	0.99
K_a	0.03	0.04	n	1.34	1.15
Q_m	144.92	370.37	K_f	6.49	14.90
χ^2	1.2	0.09	χ^2	0.26	1.13

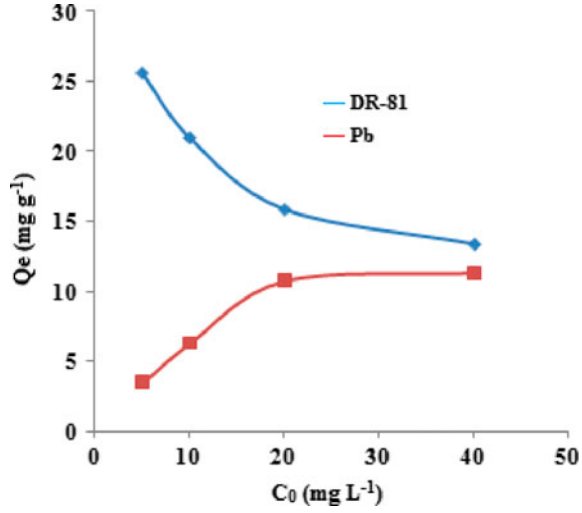

Fig. 8. Mutual effect of lead and DR-81 on adsorption property.

concentration of Pb^{2+} was constant at 5 mg L^{-1} and the concentration of DR-81 was varied. As shown at Fig. 8, by increasing the concentration of DR-81, Pb^{2+}

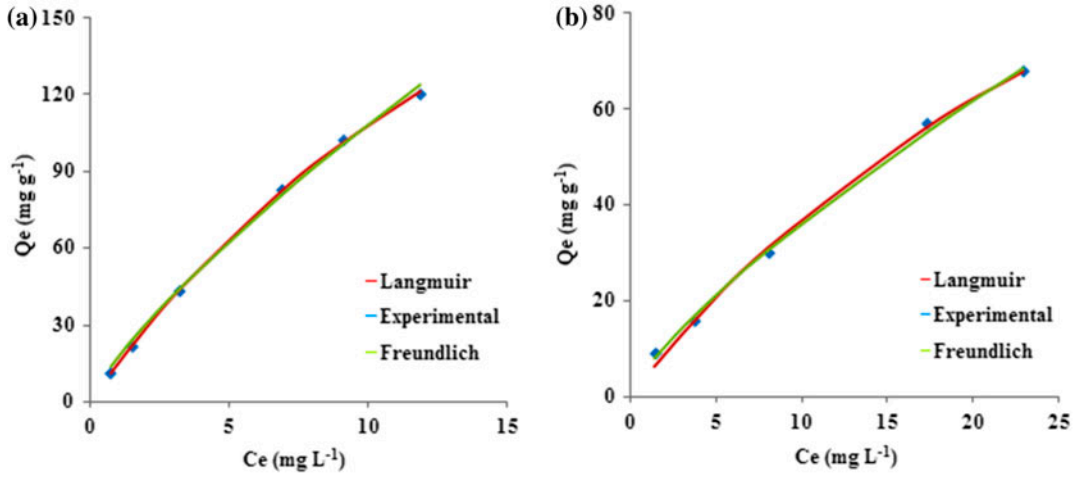

Fig. 7. Fitting calculated adsorption data with experimental values for lead (a) and DR-81 (b).

Table 3
Comparison the lead adsorption property of prepared composite with some adsorbents

Adsorbent	Capacity (mg g^{-1})	Time (min)	Refs.
Poly(o-phenylenediamine)	4,700	20 h	[11]
Poly(m-phenylenediamine)	238.9	20	[12]
Poly(o-phenylenediamine)/GO	228	100	[13]
MCM-48	127.24	90	[25]
Fe_3O_4-poly phenylenediamine	370.37	5	This work

Table 4
Comparison dye adsorption property of prepared composite with some sorbents

Adsorbent	Dye	Capacity (mg g^{-1})	Time (min)	Refs.
Waste iron ore	Congo red	172.4	30	[4]
$CuFe_2O_4$/activated carbon	Acid orange II	404	300	[5]
Orange peel carbon	Direct Yellow 12	75.76	120	[19]
Waterworks sludge	Direct blue 71	625	160	[20]
Cellulose/Fe_3O_4/activated carbon	Congo red	66.09	15 h	[27]
Fe_3O_4-poly phenylenediamine	Direct red 81	144.92	5	This work

adsorption was significantly increased this could be due to the electrostatics and chelation interactions between the heavy metal ion and anionic dye, which assist Pb^{2+} adsorption.

3.8. Regeneration of sorbent

In order to have economical adsorption process, regeneration of solid sorbent is of a great importance. To this end, release of adsorbed analytes from the sorbent surface was also investigated. According to effect of pH on lead adsorption, the removal efficiency was not quantative in acidic situations. Therefore, it can be estimated that acidic solution may be an appropriate eluent for lead desorption. As a result, different concentrations of HNO_3 solution were applied and the result showed that 0.5 mol L^{-1} could release target ions with efficiency of 95%. Moreover, adsorbed dye was released completely from sorbent surface by ethanol –NaOH (0.1 mol L^{-1}) mixture.

3.9. Comparison with other methods

In Tables 3 and 4, the performance of proposed method for lead and dye adsorption was compared with some repots in literature. Based on the results, the performance of this method was significantly better than the most previous ones with respect to the adsorption capacity and adsorption time. According to these results, the proposed system is a good candidate for environmental remediation purpose to reduce the hazardous impact of heavy metals and hazardous dyes.

4. Conclusion

In this paper, poly-phenylenediamine-eco-friendly synthesized Fe_3O_4 nanocomposite was used for DR-81 and Pb^{2+} adsorption in both single and binary systems. The adsorption processes is fast as equilibrium time was 5 min and the kinetic well fitted by pseudo-second-order kinetic model. The Freundlich isotherm could perfectly describe the adsorption processes of dye, however, lead adsorption followed Langmuir model. The maximum adsorption capacities were found to be 144.92 and 370.37 mg g^{-1} for DR-81 and Pb^{2+}, respectively. Results indicate that, magnetic nanocomposite is an effective candidate in the adsorption of heavy metals and dyes as it is cost-effective and its synthesis method is simple.

Acknowledgment

Support for this investigation by the Research Council of the University of Tehran through grants is gratefully acknowledged.

References

[1] H.Y. Zhu, R. Jiang, L. Xiao, W. Li, A novel magnetically separable γ-Fe_2O_3/ crosslinked chitosan adsorbent: Preparation, characterization and adsorption application for removal of hazardous azo dye, J. Hazard. Mater. 179 (2010) 251–257.
[2] L. Ai, H. Huang, Z. Chen, X. Wei, J. Jiang, Activated carbon/$CoFe_2O_4$ composite: Facile synthesis, magnetic performance and their potential application for the removal of malachite green from water, Chem. Eng. J. 156 (2010) 243–249.

[3] A. Mehdinia, F. Roohi, A. Jabbari, Rapid magnetic solid phase extraction with in situ derivatization of methyl mercury in sea water by Fe_3O_4/polyaniline nanoparticle, J. Chromatogr. A. 1218 (2010) 4269–4274.
[4] S.K. Giri, N.N. Das, G.C. Pradhan, Synthesis and characterization of magnetite nanoparticles using waste iron ore tailings for adsorptive removal of dyes from aqueous solution, Colloids Surf. A 389 (2011) 43–49.
[5] G. Zhang, J. Qu, H. Liu, A.T. Cooper, R. Wu, $CuFe_2O_4$/ activated carbon composite: A novel magnetic adsorbent for the removal of acid orange II, Chemosphere 68 (2007) 1058–1066.
[6] J. Prasad Rao, K.E. Geckeler, Polymer nanoparticles: Preparation techniques and size control parameters, Prog. Polym. Sci. 36 (2011) 887–913.
[7] M. Baghayeri, E. Nazarzadeh, M. Namadchian, Direct electrochemistry and electrocatalysis of hemoglobin immobilized on biocompatible poly(styrene-alternative-maleic acid)/functionalized multi-wall carbon nanotubes blends, Sens. Actuators B 188 (2013) 227–234.
[8] X.G. Li, M.R. Huang, W. Duan, Y.L. Yang, Novel multifunctional polymers from aromatic diamines by oxidative polymerizations, Chem. Rev. 102 (2002) 2925–3030.
[9] M. Baghayeri, Glucose sensing by a glassy carbon electrode modified with glucose oxidase and a magnetic polymeric nanocomposite, RSC Adv. 5 (2015) 18267–18274.
[10] M. Baghayeri, E. Nazarzadeh Zare, M.M. Lakouraj, Novel superparamagnetic PFu@Fe_3O_4 conductive nanocomposite as a suitable host for hemoglobin immobilization, Sens. Actuators B 202 (2014) 1200–1208.
[11] J. Han, J. Dai, Highly efficient adsorbents of poly(o-phenylenediamine) solid and hollow sub-microspheres towards lead ions: A comparative study, J. Colloid Interface Sci. 356 (2011) 749–756.
[12] M.R. Huang, H.J. Lu, X.G. Li, Efficient multicyclic sorption and desorption of lead ions on facilely prepared poly(m-phenylenediamine) particles with extremely strong chemoresistance, J. Colloid Interface Sci. 313 (2007) 72–79.
[13] L. Yang, Z. Li, G. Nie, Z. Zhang, X. Lu, C. Wang, Fabrication of poly(o-phenylenediamine)/reduced graphene oxide composite nanosheets via microwave heating and their effective adsorption of lead ions, Appl. Surf. Sci. 307 (2014) 601–607.
[14] M. Baghayeri, E. Nazarzadeh Zare, M.M. Lakouraj, A simple hydrogen peroxide biosensor based on aelectro magnetic poly(p-phenylenediamine)@Fe_3O_4 nanocomposite, Biosens. Bioelectron. 55 (2014) 259–265.
[15] M. Baghayeri, E. Nazarzadeh Zare, M.M. Lakouraj, Monitoring of hydrogen peroxide using a glassy carbon electrode modified with hemoglobin and a polypyrrole-based nanocomposite, Microchim. Acta 182 (2015) 771–779.
[16] M. Baghayeri, E. Nazarzadeh Zare, R. Hasanzadeh, Facile synthesis of PSMA-*g*-3ABA/MWCNTs nanocomposite as a substrate for hemoglobin immobilization: Application to catalysis of H_2O_2, Mater. Sci. Eng. C 39 (2014) 213–220.
[17] R.M. Khafagy, Synthesis, characterization, magnetic and electrical properties of the novel conductive and magnetic Polyaniline/$MgFe_2O_4$ nanocomposite having the core–shell structure, J. Alloys Compd. 509 (2011) 9849–9857.
[18] A. Mittal, J. Mittal, A. Malviya, V.K. Gupta, Adsorptive removal of hazardous anionic dye "Congo red" from wastewater using waste materials and recovery by desorption, J. Colloid Interface Sci. 340 (2009) 16–26.
[19] A. Khaled, A. El-Nemr, A. El-Sikaily, O. Abdelwahab, Treatment of artificial textile dye effluent containing Direct Yellow 12 by orange peel carbon, Desalination 238 (2009) 210–232.
[20] B. Kayranli, Adsorption of textile dyes onto iron based waterworks sludge from aqueous solution; isotherm, kinetic and thermodynamic study, Chem. Eng. J. 173 (2011) 782–791.
[21] S. Kaur, S. Rani, R. Kumar Mahajan, Adsorptive removal of dye crystal violet onto low-cost carbon produced from Eichhornia plant: Kinetic, equilibrium, and thermodynamic studies, Desalin. Water Treat. 53 (2015) 543–556.
[22] X. Ren, W. Xiao, R. Zhang, Y. Shang, R. Han, Adsorption of crystal violet from aqueous solution by chemically modified phoenix tree leaves in batch mode, Desalin. Water Treat. 53 (2015) 1324–1334.
[23] X. Hu, Y. Liu, H. Wang, G. Zeng, X. Hu, Y. Guo, T. Li, A. Chen, L. Jiang, F. Guo, Adsorption of copper by magnetic graphene oxide-supported β-cyclodextrin: Effects of pH, ionic strength, background electrolytes, and citric acid, Chem. Eng. Res. Des. 93 (2015) 675–683.
[24] Y. Li, Q. Du, T. Liu, X. Peng, J. Wang, J. Sun, Y. Wang, S. Wu, Z. Wang, Y. Xia, L. Xia, Comparative study of methylene blue dye adsorption onto activated carbon, graphene oxide, and carbon nanotubes, Chem. Eng. Res. Des. 91 (2013) 361–368.
[25] M. Anbia, K. Kargosha, S. Khoshbooei, Heavy metal ions removal from aqueous media by modified magnetic mesoporous silica MCM-48, Chem. Eng. Res. Des. 93 (2015) 779–788.
[26] W. Lu, Y. Shen, A. Xie, W. Zhang, Green synthesis and characterization of superparamagnetic Fe_3O_4 nanoparticles, J. Magn. Magn. Mater. 322 (2010) 1828–1833.
[27] H.Y. Zhu, Y.-Q. Fu, R. Jiang, J.H. Jiang, L. Xiao, G.M. Zeng, S.L. Zhao, Y. Wang, Adsorption removal of congo red onto magnetic cellulose/Fe_3O_4/activated carbon composite: Equilibrium, kinetic and thermodynamic studies, Chem. Eng. J. 173 (2011) 494–502.
[28] L.B.L. Lim, N. Priyantha, T. Zehra, C. Wei Then, C. Mei Chan, Adsorption of crystal violet dye from aqueous solution onto chemically treated Artocarpusodoratissimusskin: Equilibrium, thermodynamics, and kinetics studies, Desalin. Water Treat. 57(22) (2016) 10246–10260, doi: 10.1080/19443994.2015.1033474.
[29] R. Ahmad, Studies on adsorption of crystal violet dye from aqueous solution onto coniferous pinus bark powder (CPBP), J. Hazard. Mater. 171 (2009) 767–773.
[30] M.P. Starch, D.F. Apopei, M.V. Dinu, A.W. Trochimczuk, E.S. Dragan, Sorption isotherms of heavy metal ions onto semi-interpenetrating polymer network cryogels based on polyacrylamide and anionically modified potato starch, Ind. Eng. Chem. Res. 51 (2012) 10462–10471.